Redox-responsive Crown Ethers containing a Direct Link between the Ferrocene Redox-active Centre and a Benzo-crown Ether. Crystal Structures of a Ferrocene Benzo-15-crown-5 Ligand and of its Sodium Complex‡

Paul D. Beer*,† **and Harrison Sikanyika**
School of Chemistry, University of Birmingham, Birmingham B15 2TT
Christopher Blackburn and Jerome F. McAleer
MediSense, 38 Nuffield Way, Abingdon, Oxon OX14 1RL
Michael G. B. Drew*
Department of Chemistry, The University, Whiteknights, P.O. Box 224, Reading RG6 2AD

New redox-active crown ethers, 15-ferrocenyl-2,3,5,6,8,9,11,12-octahydro-1,4,7,10,13-benzopentaoxacyclopentadecine (L^1) and *N*-(4-ferrocenylphenyl)-1,4,7,10-tetraoxa-13-azacyclopentadecane (L^2), containing a direct link between the ferrocene redox centre and respectively benzo-15-crown-5 and *N*-phenylaza-15-crown-5, have been prepared. The sodium cation forms 1 : 1 stoicheiometric complexes with both ionophores whereas the larger potassium cation produces 1 : 2 intermolecular sandwich complexes with the same ligands, which were also observed by fast-atom-bombardment mass spectrometry. Single-crystal *X*-ray structures of L^1 and of its sodium complex $[NaL^1]PF_6$ have also been determined. Electrochemical investigations reveal that the binding of Na^+, K^+, and Mg^{2+} guest cations by L^1 and L^2 results in shifts of the respective ferrocene–ferrocenium redox couple to more positive potentials. The magnitude of these one-wave anodic shifts is related to the charge : radius ratio of the cationic guest species.

The prospect of advancing chemical sensor technology, modelling electron-transfer processes in biological systems, and producing new redox catalysts has led to considerable interest in the design and syntheses of redox-active macrocyclic receptor molecules that contain a redox centre in close proximity to a host binding site.[1] We and others have demonstrated that reducible[2–5] or oxidisable[6–10] redox-active macrocycles can electrochemically recognise cationic (metal, ammonium[11]) and anionic[12] (bromide) guest species either by 'through space' electrostatic perturbation and/or *via* various bond linkages between the heteroatoms of the ionophore and the redox centre. A combination of many factors including (*i*) redox-active host–guest complementarity, (*ii*) the polarising power of the guest, (*iii*) proximity of the host binding site to the redox centre, and (*iv*) nature of the bond linkage from the host binding site to the redox centre can contribute to the experimentally observed magnitude and type (one or two waves) of the shift in the respective redox couples of these host systems produced by charged guest binding. With respect to the last two factors we report here the synthesis, co-ordination, and electrochemistry of the first examples of a class of compound in which the ferrocene redox-active centre is *directly* linked to a benzo-crown ether moiety including the single crystal *X*-ray structures of the free host (1) and of its sodium complex. A preliminary report of this work has recently appeared.[8]

Experimental

Reactions were carried out under an atmosphere of dry nitrogen and solvents were distilled prior to use from an appropriate drying agent. Proton n.m.r. spectra were recorded at 400 and 270 MHz and ^{13}C n.m.r. spectra at 100 and 67.8 MHz using tetramethylsilane as internal standard. Microanalyses were performed by the Birmingham University School of Chemistry microanalytical service. Electrochemical measurements were performed using a PAR 174A polarographic analyser. Cyclic voltammetric measurements were carried out in acetonitrile solution containing 0.2 mol dm^{-3} $NBu^n{}_4BF_4$ as supporting electrolyte using a platinum-bead working electrode with ferrocene as internal reference. Values are quoted relative to the saturated calomel reference electrode (s.c.e.). Positive-ion fast-atom-bombardment mass spectrometry was performed using a primary atom beam of argon (6 keV, *ca.* 9.6 × 10^{-16} J) on a Kratos MS80 RF mass spectrometer coupled to a Kratos DS55 data system.

4-Aminobenzo-15-crown-5 (15-amino-2,3,5,6,8,9,11,12-octahydro-1,4,7,10,13-benzopentaoxacyclopentadecine) and *N*-4-aminophenyl-aza-15-crown-5 (*N*-4-aminophenyl-1,4,7,10-tetraoxa-13-azacyclopentadecane) were prepared using literature procedures.[13,14]

Syntheses.—*4-Ferrocenylbenzo-*15-*crown*-5 (L^1).§ 4-Aminobenzo-15-crown-5 (1.0 g, 3.53 mmol) was dissolved in concentrated hydrochloric acid (10 cm^3) and water (10 cm^3), cooled to 0 °C, and a solution of sodium nitrite (1.0 g, 14.5 mmol) in water (20 cm^3) also at 0 °C was added dropwise. After addition was complete, the solution was stirred at 0 °C for 1 h before use.

Ferrocene (2.0 g, 10.75 mmol) was dissolved in concentrated sulphuric acid (30 cm^3) and stirred in air for 6 h. The ferrocenium ion solution was poured onto ice–water (120 cm^3) and allowed to warm to room temperature. Copper powder (1.0 g) was added and the mixture was poured onto the above diazonium ion solution. The reaction mixture was stirred at 0 °C for 30 min after which time the cooling bath was removed and stirring continued at room temperature for 40 h.

---

† *Present address*: Inorganic Chemistry Laboratory, University of Oxford, South Parks Road, Oxford OX1 3QR.

‡ *Supplementary data available*: see Instructions for Authors, *J. Chem. Soc., Dalton Trans.*, 1990, Issue 1, pp. xix—xxii.

§ 15-Ferrocenyl-2,3,5,6,8,9,11,12-octahydro-1,4,7,10,13-benzopentaoxacyclopentadecine.

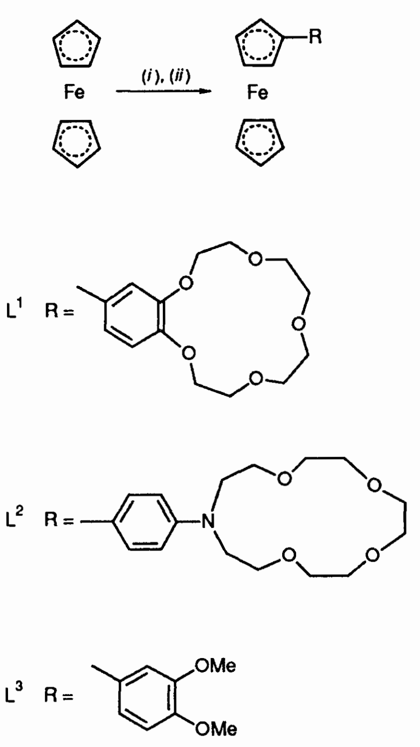

Scheme 1. (*i*) H^+; (*ii*) $RN_2^+Cl^-$

Excess of ascorbic acid (6.0 g) was added followed by dichloromethane (200 cm^3) and the mixture filtered through Celite. The residue was washed several times with dichloromethane. The washings were combined with several dichloromethane extracts of the aqueous layer and dried ($MgSO_4$). The crude product obtained after removal of the solvent was chromatographed on a silica gel 60 column, eluting with a light petroleum (60—80 °C)—dichloromethane gradient. The first band to be eluted with 100% light petroleum gave recovered ferrocene (1.25 g). The second band eluted with petroleum–dichloromethane (75:25) afforded the monosubstituted ferrocene L^1 (0.45 g, 30% yield) as orange crystals, m.p. 110—112 °C, *m/z* 452. ^1H n.m.r. ($CDCl_3$); δ 3.75—3.90 (m, 16 H, OCH_2CH_2), 4.00 (s, 5 H, unsubstituted C_5H_5 ring), 4.20—4.30 (t, *J* 1.7, 2 H, ferrocenyl H), 4.50—4.60 (t, *J* 1.7 Hz, 2 H, ferrocenyl H), and 6.81—7.12 (m, 3 H, aryl H) (Found: C, 62.8; H, 6.5. Calc. for $C_{24}H_{28}FeO_5$: C, 63.7; H, 6.2%).

N-(4-Ferrocenylphenyl)-aza-15-crown-5 (L^2) * and the model compound L^3 were prepared by procedures analogous to that described for L^1. Compound L^2 25% yield, m.p. 95 °C, *m/z* 479; ^1H n.m.r. ($CDCl_3$) δ 3.55—3.80 (m, 20 H, OCH_2), 4.20 (s, 5 H, ferrocenyl H), 4.20 (t, 2 H, $J = 2$, ferrocenyl H), 4.32 (t, 2 H, $J = 2$, ferrocenyl H), 6.62 (d, 2 H, $J = 9$, aryl H), and 7.24 (d, 2 H, $J = 9$ Hz, aryl H) (Found: C, 64.8; H, 6.7; N, 2.6. Calc. for $C_{26}H_{33}FeNO_4$: C, 65.1; H, 6.9; N, 2.9%). Compound L^3: 20% yield, m.p. 99—100 °C, *m/z* 322; ^1H n.m.r. ($CDCl_3$) δ 3.81 (s, 6 H, OCH_3), 4.05 (s, 5 H, ferrocenyl H), 4.27 (t, $J = 2$, 2 H, ferrocenyl H), 4.55 (t, $J = 2$ Hz, 2 H, ferrocenyl H), and 6.75—7.25 (m, 3 H, aryl H) (Found: C, 67.3; H, 6.1. Calc. for $C_{18}H_{18}FeO_2$: C, 67.1; H, 5.6%).

Sodium and potassium complexes of L^1 *and* L^2. To a methanolic solution of either L^1 or L^2 (1 mmol) was added an excess amount of alkali-metal hexafluorophosphate salt (5 mmol). The resulting solution was refluxed for 30 min, and upon cooling an orange precipitate was collected and dried *in vacuo*. Recrystallisation from methanol gave the respective complexes in quantitative yields: $[NaL^1]PF_6{\cdot}2H_2O$ (Found: C, 43.8; H, 4.8. Calc. for $C_{24}H_{32}F_6FeNaO_7P$: C, 43.8; H, 4.9%); $[KL^1{}_2]PF_6$ (Found: C, 52.7; H, 5.1. Calc. for $C_{48}H_{56}F_6Fe_2KO_{10}P$: C, 52.9; H, 5.2%); $[NaL^2]PF_6{\cdot}H_2O$ (Found: C, 46.5; H, 5.1; N, 2.0. Calc. for $C_{26}H_{35}F_6FeNNaO_5P$: C, 46.9; H, 5.3; N, 2.1%); $[KL^2{}_2]PF_6$ (Found: C, 54.2; H, 5.4; N, 2.6. Calc. for $C_{52}H_{66}F_6Fe_2KN_2O_8P$: C, 54.6; H, 5.8; N, 2.5%).

Crystallography.—Crystal data. L^1, $C_{24}H_{28}FeO_5$, $M = 452.1$, monoclinic, space group $P2_1/c$, $a = 13.469(11)$, $b = 7.753(9)$, $c = 20.810(13)$ Å, $\beta = 103.0(1)°$, $U = 2\,117.3$ $Å^3$, $F(000) = 952$, $D_m = 1.45$ g cm^{-3}, $Z = 4$, $D_c = 1.42$ g cm^{-3}, Mo-K_α radiation ($\lambda = 0.7107$ Å), μ(Mo-K_α) = 7.67 cm^{-1}.

$[NaL^1]PF_6$, $C_{24}H_{28}F_6FeNaO_5$, $M = 620.0$, monoclinic, space group $C2/c$, $a = 18.511(15)$, $b = 7.666(8)$, $c = 38.758(25)$ Å, $\beta = 103.0(1)°$, $U = 5\,359.0$ $Å^3$, $F(000) = 2\,544$, $D_m = 1.53$ g cm^{-3}, $Z = 8$, $D_c = 1{,}56$ g cm^{-3}, Mo-K_α radiation ($\lambda = 0.7107$ Å), μ(Mo-K_α) = 7.47 cm^{-1}.

Crystals of approximate size 0.3 × 0.3 × 0.3 mm for L^1 and 0.4 × 0.2 × 0.2 mm for $[NaL^1]PF_6$ were set up to rotate about the *b* axes on a Stoe Stadi2 diffractometer and data were collected *via* variable-width ω scans. Background counts were for 20 s and a scan rate of 0.0333° s^{-1} was applied to a width of $(1.5 + \sin \mu/\tan\theta)$. For L^1 3 033 and for $[NaL^1]PF_6$ 5 673 independent reflections were measured with a 2θ maximum of 50° of which 1 705 and 1 751 with $I > 2\sigma(I)$ were used in subsequent refinement. Both structures were solved by heavy-atom methods. In L^1 several of the atoms in the benzo-15-crown-5 were disordered over two positions and these were subsequently refined with individual occupancy factors, constrained where appropriate. Atoms in the region of the disorder were given isotropic thermal parameters but otherwise all non-hydrogen atoms in the structures were refined anisotropically. Hydrogen atoms were placed in appropriate trigonal or tetrahedral positions and refined using four common thermal parameters. The final *R* values were for L^1 0.083 ($R' = 0.093$) and for $[NaL^1]PF_6$ 0.080 ($R' = 0.092$). Both structures were given a weighting scheme in the form $w = 1/[\sigma^2(F) + 0.003F^2]$. Calculations were carried out using SHELX 76[15] and some of our own programs on the Amdahl V7 computer at the University of Reading. In the last cycle of refinement no shift was greater than 0.2σ and in the final Fourier difference map there were no significant peaks (L^1, maximum 0.42, minimum −0.40; in $[NaL^1]PF_6$, maximum 0.62, minimum −0.45 e $Å^3$). Positional parameters are given in Tables 1 and 2 and molecular dimensions in the metal co-ordination spheres are listed in Tables 3 and 4. Torsion angles in the benzo-15-crown-5 ring are given in Table 5.

Additional material available from the Cambridge Crystallographic Data Centre comprises H-atom co-ordinates, thermal parameters, and remaining bond lengths and angles.

Results and Discussion

Syntheses.—Compound L^1—L^3 were prepared using the method of Weinmayr[16] for the synthesis of arylferrocenes. Dissolving ferrocene in concentrated sulphuric acid initially produces the ferrocenium ion which, on treatment with the diazonium salt of the appropriate aromatic amine[13,14] and subsequent careful column chromatographic purification gave respective 30, 25, and 20% yields of L^1, L^2, and L^3 (Scheme 1). The structures of these new air-stable orange crystalline compounds were characterised by elemental analyses, mass spectrometry, and ^1H n.m.r. spectroscopy (see Experimental section).

---

* *N*-(4-ferrocenylphenyl)-1,4,7,10-tetraoxa-13-azacyclopentadecane.

Table 1. Atomic co-ordinates for L^1 ($\times 10^4$) with estimated standard deviations in parentheses

Atom	x	y	z	Atom	x	y	z
Fe	8 364(1)	5 598(2)	3 237(1)	O(31)	4 907(5)	10 230(8)	4 049(4)
C(11)	8 216(6)	8 188(9)	3 246(5)	C(32)	5 426(8)	11 869(11)	4 078(6)
C(12)	7 232(7)	7 406(13)	2 865(5)	C(33)	5 081(10)	12 904(11)	4 610(6)
C(13)	7 460(8)	6 438(14)	2 346(4)	O(34)	4 030(6)	13 351(8)	4 382(5)
C(14)	8 501(9)	6 588(15)	2 353(6)	C(35)	3 359(13)	12 861(18)	4 775(8)
C(15)	8 907(7)	7 726(13)	2 897(5)	C(36A)	2 825(22)	11 460(41)	4 576(15)
C(1)	8 834(12)	3 061(14)	3 343(8)	C(36B)	2 284(24)	12 369(50)	4 512(16)
C(2)	7 842(8)	3 193(10)	3 403(6)	O(37)	1 927(11)	11 271(20)	4 929(7)
C(3)	7 806(10)	4 315(11)	3 921(7)	C(38A)	1 058(28)	10 687(40)	4 526(21)
C(4)	8 803(9)	4 768(14)	4 170(6)	C(38B)	1 525(20)	9 566(28)	4 934(14)
C(5)	9 481(9)	4 043(13)	3 856(7)	C(39)	950(12)	8 785(23)	4 382(8)
C(21)	6 248(5)	7 502(10)	3 060(4)	O(40A)	1 533(11)	8 604(20)	3 890(7)
C(22)	6 032(5)	8 894(9)	3 443(4)	O(40B)	1 965(25)	7 605(52)	4 385(19)
C(23)	5 180(5)	8 922(9)	3 667(4)	C(41A)	2 029(20)	6 948(27)	4 021(14)
C(24)	4 447(8)	7 716(14)	3 479(5)	C(41B)	1 706(28)	7 200(53)	3 751(19)
C(25)	4 627(7)	6 303(15)	3 078(5)	C(42)	2 705(9)	6 632(15)	3 482(7)
C(26)	5 528(6)	6 227(14)	2 875(4)	O(43)	3 560(6)	7 810(11)	3 711(4)

Table 2. Atomic co-ordinates for [NaL^1]PF$_6$ ($\times 10^4$) with estimated standard deviations in parentheses

Atom	x	y	z	Atom	x	y	z
Fe	3 355(1)	5 015(2)	1 988(0)	C(32)	4 032(11)	3 946(16)	3 575(4)
Na	4 763(3)	7 140(7)	4 168(1)	C(33)	4 126(11)	3 309(17)	3 951(3)
C(1)	3 409(7)	2 354(12)	2 014(4)	O(34)	4 813(7)	3 910(12)	4 137(3)
C(2)	4 069(7)	3 131(17)	2 214(4)	C(35)	4 976(12)	3 359(21)	4 490(4)
C(3)	4 387(7)	4 128(18)	1 993(4)	C(36)	5 733(12)	4 178(25)	4 669(5)
C(4)	2 954(15)	3 987(28)	1 643(4)	O(37)	5 657(7)	5 989(18)	4 655(3)
C(5)	3 381(12)	2 888(31)	1 679(7)	C(38)	6 354(10)	6 888(32)	4 739(4)
C(11)	3 311(7)	7 713(16)	2 011(3)	C(39)	6 170(13)	8 844(34)	4 678(5)
C(12)	3 242(8)	6 973(15)	2 330(3)	O(40)	5 791(6)	9 144(17)	4 320(3)
C(13)	2 582(6)	5 864(18)	2 252(3)	C(41)	6 167(9)	9 324(27)	4 083(5)
C(14)	2 282(9)	5 971(18)	1 873(3)	C(42)	5 708(8)	9 763(21)	3 721(4)
C(15)	2 767(8)	7 059(15)	1 747(3)	O(43)	5 095(5)	8 389(12)	3 655(2)
C(21)	3 732(7)	7 356(15)	2 671(3)	P	3 190(3)	8 697(6)	4 334(1)
C(22)	3 716(6)	6 397(16)	2 976(3)	F(1)	3 500(8)	9 002(15)	3 983(3)
C(23)	4 156(8)	6 767(14)	3 303(3)	F(2)	2 922(8)	8 450(21)	4 677(3)
C(24)	4 652(7)	8 241(14)	3 326(3)	F(3)	3 156(11)	10 708(18)	4 380(5)
C(25)	4 701(8)	9 262(19)	3 040(4)	F(4)	3 282(17)	6 773(22)	4 286(7)
C(26)	4 233(6)	8 835(13)	2 739(4)	F(5)	2 391(9)	8 762(36)	4 140(3)
O(31)	4 178(5)	5 861(11)	3 604(2)	F(6)	3 971(8)	8 730(41)	4 525(4)

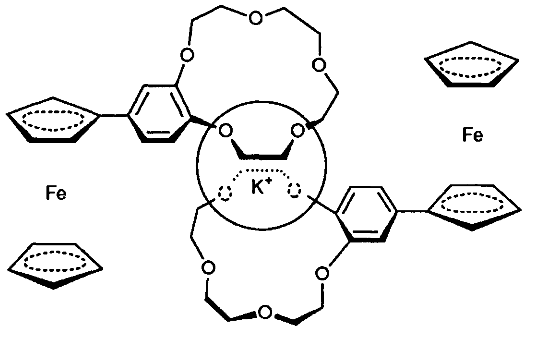

Scheme 2.

Co-ordination Studies.—The co-ordination properties of L^1 and L^2 were investigated by refluxing aqueous methanolic solutions of the respective ligand with an excess amount of sodium or potassium hexafluorophosphate. Upon cooling deep orange crystals were isolated whose elemental analyses were determined. The sodium cation was found to form 1:1 alkali-metal cation:ligand complexes with both ionophores whereas the larger potassium cation forms 1:2 alkali-metal cation: ligand complexes (Scheme 2). These stoicheiometric formulations were also detected by fast-atom-bombardment (f.a.b.) mass spectrometry.

X-Ray Structural Investigations of L^1 *and* [NaL^1]PF$_6$.—Slow evaporation of aqueous methanolic solutions of L^1 and [NaL^1]PF$_6$ led to the respective isolation of orange crystallographic quality crystals whose *X*-ray crystal structures were determined.

The structures consisting of discrete molecules of L^1 and [NaL^1]PF$_6$ are compared in Figure 1 which shows identical projections with respect to the benzene rings. As can be seen there are several discernible differences between the two structures. Starting from the benzene ring, the angle to the attached cyclopentadiene ring is 23.3 in L^1 but only 14.5° in [NaL^1]PF$_6$. The two five-membered rings intersect at an angle of 5.9 in L^1 but only 2.5° in [NaL^1]PF$_6$. In L^1 the Fe–C bond lengths range from 1.997(9) to 2.112(11) Å while in [NaL^1]PF$_6$ distances range from 2.014(12) to 2.076(24) Å. In both structures (Figure 1) the ferrocene geometry is intermediate between staggered and eclipsed.

The conformation of the benzo-15-crown-5 section of the structures also differs considerably though the variations are difficult to analyse in detail because of the disorder in L^1. However it is clear that in [NaL^1]PF$_6$ the five oxygen atoms are

Table 3. Molecular dimensions (distances in Å, angles in °) around Fe for L^1 and $[NaL^1]PF_6$

	L^1	$[NaL^1]PF_6$
Fe–C(1)	2.063(12)	2.043(10)
Fe–C(2)	2.049(8)	2.019(13)
Fe–C(3)	2.015(13)	2.024(14)
Fe–C(4)	2.003(11)	2.076(24)
Fe–C(5)	2.122(11)	2.029(25)
C(1)–Fe–C(2)	39.0(5)	41.0(5)
C(1)–Fe–C(3)	67.0(5)	68.2(5)
C(2)–Fe–C(3)	40.2(4)	39.7(6)
C(1)–Fe–C(4)	64.8(5)	68.0(7)
C(2)–Fe–C(4)	65.3(5)	67.4(7)
C(3)–Fe–C(4)	39.9(5)	40.4(7)
C(1)–Fe–C(5)	40.1(5)	38.7(8)
C(2)–Fe–C(5)	66.7(4)	65.2(7)
C(3)–Fe–C(5)	67.5(5)	65.7(7)
C(4)–Fe–C(5)	38.3(5)	39.5(9)
C(1)–Fe–C(11)	167.5(5)	174.9(5)
C(2)–Fe–C(11)	149.9(4)	136.4(5)
C(3)–Fe–C(11)	115.5(4)	112.4(5)
C(4)–Fe–C(11)	108.6(4)	116.0(7)
C(5)–Fe–C(11)	128.1(4)	146.4(8)
C(1)–Fe–C(12)	149.4(5)	135.5(5)
C(2)–Fe–C(12)	115.1(4)	113.4(5)
C(3)–Fe–C(12)	103.7(4)	118.3(5)
C(4)–Fe–C(12)	127.4(4)	147.5(7)
C(5)–Fe–C(12)	164.9(5)	172.7(8)
C(11)–Fe–C(12)	43.1(5)	39.5(5)
C(1)–Fe–C(13)	119.9(5)	109.0(5)
C(2)–Fe–C(13)	106.3(4)	118.3(6)
Fe–C(11)	2.018(8)	2.073(12)
Fe–C(12)	2.088(10)	2.043(13)
Fe–C(13)	2.081(10)	2.044(14)
Fe–C(14)	2.040(11)	2.069(15)
Fe–C(15)	1.997(9)	2.014(12)
C(3)–Fe–C(13)	123.2(4)	150.2(5)
C(4)–Fe–C(13)	161.8(4)	168.3(6)
C(5)–Fe–C(13)	155.7(5)	131.5(7)
C(11)–Fe–C(13)	70.0(4)	67.8(5)
C(12)–Fe–C(13)	39.4(4)	42.0(5)
C(1)–Fe–C(14)	111.6(5)	113.5(5)
C(2)–Fe–C(14)	126.8(5)	148.2(5)
C(3)–Fe–C(14)	161.2(5)	168.3(6)
C(4)–Fe–C(14)	158.1(5)	128.4(6)
C(5)–Fe–C(14)	124.4(5)	107.8(6)
C(11)–Fe–C(14)	70.3(4)	67.1(5)
C(12)–Fe–C(14)	67.6(4)	69.3(5)
C(13)–Fe–C(14)	39.8(4)	41.3(5)
C(1)–Fe–C(15)	134.2(4)	144.6(5)
C(2)–Fe–C(15)	167.9(4)	172.1(6)
C(3)–Fe–C(15)	151.9(4)	132.6(6)
C(4)–Fe–C(15)	123.8(4)	108.0(6)
C(5)–Fe–C(15)	114.7(4)	115.7(7)
C(11)–Fe–C(15)	39.3(3)	38.8(4)
C(12)–Fe–C(15)	67.0(4)	66.7(5)
C(13)–Fe–C(15)	67.3(4)	67.5(5)
C(14)–Fe–C(15)	41.8(4)	39.8(5)

Table 4. Molecular dimensions (distances in Å, angles in °) around Na in $[NaL^1]PF_6$

Na–O(31)	2.418(9)	Na–O(43)	2.405(11)
Na–O(34)	2.481(11)	Na–F(1)	2.695(14)
Na–O(37)	2.383(12)	Na–F(4)	2.893(33)
Na–O(40)	2.414(13)	Na–F(6)	2.542(21)
O(31)–Na–O(34)	64.29(31)	O(43)–Na–F(6)	123.0(6)
O(31)–Na–O(37)	131.03(43)	F(1)–Na–F(6)	47.1(4)
O(34)–Na–O(37)	69.02(41)	F(4)–Na–F(6)	43.7(4)
O(31)–Na–O(40)	130.36(41)	O(31)–Na–F(1)	77.8(3)
O(34)–Na–O(40)	127.67(46)	O(34)–Na–F(1)	123.7(4)
O(37)–Na–O(40)	70.90(44)	O(37)–Na–F(1)	144.4(5)
O(31)–Na–O(43)	63.95(32)	O(40)–Na–F(1)	108.5(4)
O(34)–Na–O(43)	109.79(40)	O(43)–Na–F(1)	86.4(4)
O(37)–Na–O(43)	122.75(46)	F(4)–Na–F(1)	45.3(5)
O(40)–Na–O(43)	67.36(35)	O(31)–Na–F(4)	81.7(6)
O(31)–Na–F(6)	119.39(44)	O(34)–Na–F(4)	87.6(5)
O(34)–Na–F(6)	122.4(7)	O(37)–Na–F(4)	110.7(6)
O(37)–Na–F(6)	97.4(5)	O(40)–Na–F(4)	138.3(5)
O(40)–Na–F(6)	94.7(6)	O(43)–Na–F(4)	126.6(5)

Table 5. Torsion angles (°) in the benzo-15-crown-5

	L^1 *	$[NaL^1]PF_6$
O(31)–C(23)–C(24)–O(43)	−4.5	3.5
C(32)–O(31)–C(23)–C(24)	−157.5	−165.1
C(33)–C(32)–O(31)–C(23)	−171.5	177.8
O(34)–C(33)–O(32)–O(31)	−69.1	−51.9
C(35)–O(34)–C(33)–C(32)	124.2	−178.3
C(36)–C(35)–O(34)–C(33)	−100.2	−177.6
O(37)–C(36)–C(35)–O(34)	−166.0	62.0
C(38)–O(37)–C(36)–C(35)	138.1	−166.7
C(39)–C(38)–O(37)–C(36)	72.7	175.0
O(40)–C(39)–C(38)–O(37)	−73.0	−59.3
C(41)–O(40)–C(39)–C(38)	150.9	−83.5
C(42)–C(41)–O(40)–C(39)	179.7	−175.8
O(43)–C(42)–C(41)–O(40)	73.8	−50.9
C(24)–O(43)–C(42)–C(41)	166.1	−169.4
C(23)–C(24)–O(43)–C(42)	174.7	174.1

* Disordered values quoted are from the most popular conformation.

directed inwards and thus encapsulate the sodium ion which is bound to all five oxygens as well as to three fluorine atoms of the PF_6^- anion (Figure 2).

The Na–O distances range from 2.383(12) to 2.481(11) Å. The sodium ion lies to one side of the 15-crown-5 ring at 0.88 Å above the least-squares plane of the five oxygen atoms. These atoms are not coplanar, the maximum deviation from the plane being 0.32 Å. On the opposite side the sodium ion is bonded to three fluorines atoms of the PF_6^- anion with bond lengths of 2.542(21), 2.695(14), and 2.893(33) Å. This arrangement suggests that the sodium ion is too large to fit into the cavity of benzo-15-crown-5. We located several structures in the Cambridge Crystallographic Database containing sodium ions and benzo-15-crown-5.[17–22] In many of these the arrangement of the sodium ions and the crown is equivalent to that found in the present structure. Thus in sodium picrate–benzo-15-crown-5,[17,18] the Na–O distances are 2.403, 2.456, 2.455, 2.436, and 2.507 Å; the sodium ion is 0.90 Å above the plane of the five oxygen atoms (maximum deviation of an oxygen atom from the plane 0.34 Å) and is bonded to the picrate anion on the opposite side to the crown through an *ortho* nitro group and the phenoxide oxygen atom of the picrate. In benzo-15-crown-5–sodium iodide monohydrate[19] the Na–O distances range from 2.354 to 2.427 Å and the sodium atom is 0.75 Å to one side of the O_5 plane. Similar distances and geometries are also observed in bis[(benzo-15-crown-5)sodium] tetrachlorodioxouranate,[20] bis[(benzo-15-crown-5)sodium] bis[(μ-chlorodichlorocuprate(I)],[21] and (benzo-15-crown-5)sodium bis(η-cyclo-

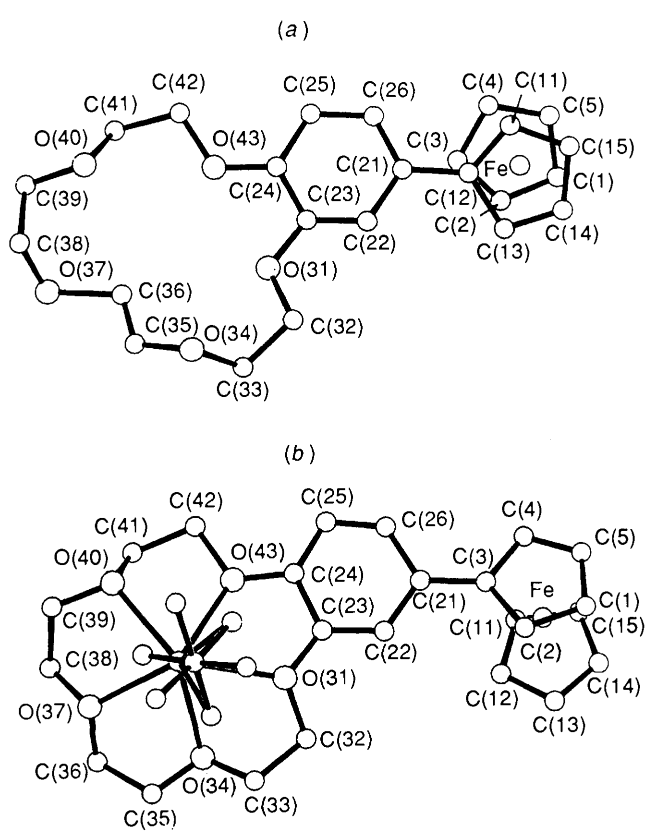

Figure 1. A comparison between the structures of (*a*) L^1 and (*b*) $[NaL^1]PF_6$

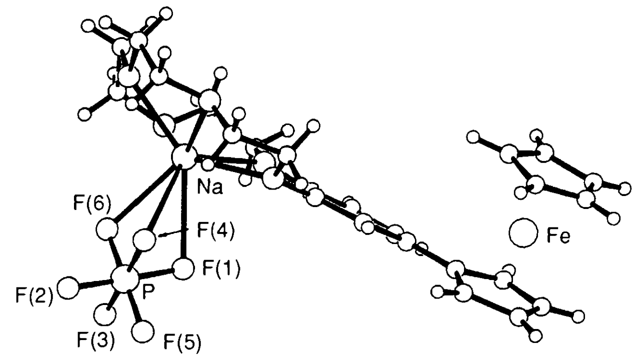

Figure 2. A view of the structure of $[NaL^1]PF_6$

Table 6. Electrochemical data

	L^1	L^2	L^3
$E_f{}^a$/V	+0.54	+0.58	+0.55
$\Delta E_p{}^b$/mV	80	80	80
$\Delta E(Na^+)^c$/mV	60	90	< 10
$\Delta E(K^+)^c$/mV	20	40	< 10
$\Delta E(Mg^{2+})^c$/mV	70	110	< 10

[a] Obtained in MeCN solution containing 0.2 mol dm^{-3} $NBu^n{}_4BF_4$ as supporting electrolyte. Solutions were *ca.* 2×10^{-3} mol dm^{-3} in complex and potentials were determined with reference to the s.c.e. [b] Separation between anodic and cathodic peak potentials of cyclic voltammograms; values for ferrocene under the same conditions ranged from 75 to 85 mV. [c] Shift in oxidation potential produced by the presence of metal cations, (4 equivalents) added as their hexafluorophosphate salts for sodium and potassium and thiocyanate salt for magnesium.

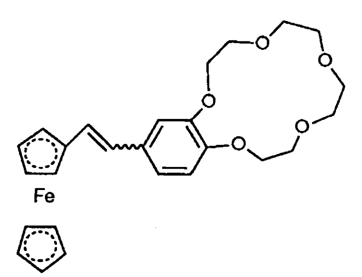

L^4 *cis*
L^5 *trans*

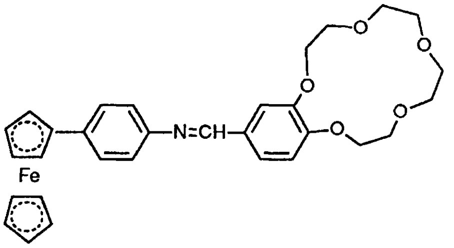

L^6

pentadienyl)dihydridoniobate.[22] In (benzo-15-crown-5)sodium perchlorate the Na–O bond lengths range from 2.373(5) to 2.464(5) Å.[23] All these structures confirm the view that the sodium ion is too large to fit into the cavity of the 15-crown-5 macrocycle. We note that conversely the size of the sodium ion is rather small to fit into the larger 18-crown-6 macrocycle as it forms short and long Na–O contacts.[24]

In all these 1:1 structures the metal ion is *ca.* 0.7—0.9 Å to one side of the 15-crown-5 ligand. There are however two structures, bis(benzo-15-crown-5)sodium perchlorate and bis(benzo-15-crown-5)sodium tetraphenylborate, where the sodium ion forms a 1:2 complex in which it is sandwiched between the two crowns.[23]

We were only to find one precedent for the bonding of the sodium ion to fluorine atoms of $PF_6{}^-$. This was (dibenzo-36-crown-12)-sodium hexafluorophosphate (1/2)[25] in which the sodium ion is bonded to two fluorine atoms at 2.528 and 2.424 Å (dibenzo-36-crown-12 = 6,7,9,10,12,13,15,16,18,19,26,27,29,30,32,33,35,36,38,39-eicosahydrodibenzo[*b*,*t*]-1,4,7,10,13,16,19,22,25,28,31,34-dodecaoxacyclohexatricontine).

Electrochemical Studies.—The electrochemical properties of compounds L^1—L^3 were investigated in acetonitrile using cyclic voltammetry with $NBu^n{}_4BF_4$ as the supporting electrolyte. Each compound exhibited a reversible redox oxidation wave in the 0.4—0.45 V region (*versus* s.c.e.) typical of a substituted ferrocene derivative (Table 6). Cyclic voltammograms were also recorded after progressively adding stoicheiometric equivalents of Na^+, K^+, or Mg^{2+} to the electrochemical solutions, and the results are summarised in Table 6.

Only in the case of L^1 and L^2 are significant one-wave anodic shifts produced with the three cationic guests, suggesting the benzo-crown ether is essential for observing cationic electrochemical recognition. This one-wave anodic shift behaviour also suggests low values of the binding constants K_1,[26] and that the rate of decomplexation k_1 of $FcIM^{n+}$ (where Fc stands for the ferrocene redox moiety and I the appended crown ether) is fast on the cyclic voltammetric time-scale (Scheme 3). It is noteworthy that the magnitude of these shifts reflects the differring polarisabilities of the bound metal cations; Mg^{2+}

$$\begin{tikzcd}
\mathrm{FcI} + \mathrm{M}^{n+} \arrow[r, shift left, "K_1"] \arrow[d, shift left] \arrow[d, phantom, "E_{1f}", shift right=4ex] & \mathrm{FcIM}^{n+} \arrow[l, shift left] \arrow[d, shift left] \arrow[d, phantom, "E_{1c}", shift left=4ex] \\
\mathrm{Fc}^{+}\mathrm{I} + \mathrm{M}^{n+} \arrow[r, shift left, "K_2"] \arrow[u, shift left] & \mathrm{Fc}^{+}\mathrm{IM}^{n+} \arrow[l, shift left] \arrow[u, shift left]
\end{tikzcd}$$

Scheme 3. Redox and complexation equilibria for a ferrocene-substituted ionophore. M′I; f denotes free (uncomplexed) ionophore, c denotes complexed species; $K_j = k_j/k_j$.

possessing the largest charge: radius ratio produces the greatest value of the anodic shift and K^+ the smallest. These experimental observations are in agreement with those found with the *cis* and *trans* olefinic linked ferrocenyl ionophores L^4, L^5 (ref. 9) and the Schiff-base linked analogue L^6.[27] Interestingly the absolute magnitudes of the anodic shifts of the respective ferrocene–ferrocenium redox couples of the three redox ionophoric systems produced by Group 1A and 2A metal cation binding are similar. For example with Mg^{2+} the respective ΔE values for L^1, L^4, and L^6 are 70, 70, and 60 mV. The predicted diminishing electrostatic perturbation ΔE values for a given cationic guest species in the order $L^1 > L^4 > L^6$, reflecting the increasing bond distance from the redox centre to the crown ether binding site, is not observed. Thus, provided a conjugated bond linkage connects the ferrocene redox centre to the host crown ether binding site, cationic electrochemical recognition will be exhibited.

Conclusion

Two new redox-active crown ethers in which a ferrocene redox centre is directly linked to respective benzo-15-crown-5 and *N*-phenylaza-15-crown-5 cation binding moieties have been synthesised. Electrochemical investigations reveal both ionophores electrochemically to recognise sodium, potassium, and magnesium guest cations by electrostatically perturbing the respective ferrocene–ferrocenium redox couple to more positive potentials. The charge: radius ratio or polarising power of the guest cation is of paramount importance in determining the magnitude of the shift in redox potential of the ferrocenyl redox centre.

Acknowledgements

We thank the British Council for financial support of this work, MediSense for additional financial support, and the S.E.R.C. for use of the high-field n.m.r. service at the University of Warwick. We are also grateful to A. W. Johans for assistance with the crystallographic investigations.

References

1 P. D. Beer, *Chem. Soc. Rev.*, 1989, **18**, 409.
2 N. Al-Obaidi, P. D. Beer, J. P. Bright, C. J. Jones, J. A. McCleverty, and S. S. Salam, *J. Chem. Soc., Chem. Commun.*, 1986, 239.
3 R. E. Wolf, jun., and S. R. Cooper, *J. Am. Chem. Soc.*, 1984, **106**, 4646.
4 L. Echegoyen, D. A. Gustowski, V. J. Gatto, and G. W. Gokel, *J. Chem. Soc., Chem. Commun.*, 1986, 220.
5 D. A. Gustowski, L. Echegoyen, D. M. Goli, A. Kaifer, R. A. Schultz, and G. W. Gokel, *J. Am. Chem. Soc.*, 1984, **106**, 1633.
6 P. D. Beer, *J. Chem. Soc., Chem. Commun.*, 1985, 1115.
7 T. Saji, *Chem. Lett.*, 1986, 275.
8 P. D. Beer, H. Sikanyika, C. Blackburn, J. F. McAleer, and M. G. B. Drew, *J. Organomet. Chem.*, 1988, **356**, C19.
9 P. D. Beer, C. Blackburn, J. F. McAleer, and H. Sikanyika, *Inorg. Chem.*, 1990, **29**, 378.
10 E. Fu, J. Grannell, M. L. H. Green, V. J. Lowe, S. R. Marder, G. C. Saunders, and M. Tuddenham, *J. Organomet. Chem.*, 1988, **355**, 205.
11 P. D. Beer, D. B. Crowe, and B. Main, *J. Organomet. Chem.*, 1989, **375**, C35.
12 P. D. Beer and A. D. Keefe, *J. Organomet. Chem.*, 1989, **375**, C40.
13 R. Ungaro, B. El. Haj, and J. Smid, *J. Am. Chem. Soc.*, 1977, **98**, 5198.
14 J. P. Dix and F. Vogtle, *Chem. Ber.*, 1980, **113**, 457.
15 G. M. Sheldrick, SHELX 76, Package for Crystal Structure Determination, University of Cambridge, 1976.
16 V. Weinmayr, *J. Am. Chem. Soc.*, 1955, **77**, 3012.
17 D. L. Ward, A. I. Popov, and N. S. Poonia, *Acta Crystallogr., Sect. C*, 1984, **40**, 238.
18 J. Xianglin, T. Yougi, W. Yangjie, A. Haoyun, and H. Hongwen, *Chem. J. Chin. Univ.*, 1985, **6**, 1051.
19 M. A. Bush and M. R. Truter, *J. Chem. Soc., Perkin Trans. 2*, 1972, 341.
20 D. C. Moody and R. R. Ryan, *Cryst. Struct. Commun.*, 1979, **8**, 933.
21 W. Dreissig, Z. Dauter, A. Cygan, and J. F. Biernat, *Inorg. Chim. Acta*, 1985, **96**, 21.
22 D. A. Lememovskii, I. E. Nifant'ev, I. F. Urazowski, E. G. Perevalova, T. V. Timofeeva, Yu. L. Slovokhotov, and Yu. T. Struchkov, *J. Organomet. Chem.*, 1988, **342**, 31.
23 J. D. Owen, *J. Chem. Soc., Dalton Trans.*, 1980, 1066.
24 G. Weber, G. M. Sheldrick, T. Burgemeister, F. Dietl, A. Mannschreck, and A. Merz, *Tetrahedron*, 1984, **40**, 855.
25 J. M. Maud, J. F. Stoddart, H. M. Colquhoun, and D. J. Williams, *Polyhedron*, 1984, **3**, 675.
26 S. R. Miller, D. A. Gustowski, Z. Chen, G. W. Gokel, L. Echegoyen, and A. Kaifer, *Anal. Chem.*, 1988, **60**, 2021.
27 P. D. Beer and H. Sikanyika, *Polyhedron*, 1990, **9**, 1091.

Received 25*th April* 1990; *Paper* 0/01840F